Available online at www.sciencedirect.com
SCIENCE DIRECT
Solid State Communications 137 (2006) 381–386
solid state communications
www.elsevier.com/locate/ssc

Reduced dielectric loss and leakage current in $CaCu_3Ti_4O_{12}/SiO_2/CaCu_3Ti_4O_{12}$ multilayered films

Liang Fang [a,*], Mingrong Shen [a], Jing Yang [a], Zhenya Li [a,b]

[a] Department of Physics and Jiangsu Key Laboratory of Thin Films, Suzhou University, Suzhou 215006, People's Republic of China
[b] CCAST (World Laboratory), P.O. Box 8730, Beijing 100080, People's Republic of China

Received 6 September 2005; received in revised form 1 December 2005; accepted 5 December 2005 by T.M.M. Palstra
Available online 22 December 2005

Abstract

The $CaCu_3Ti_4O_{12}/SiO_2/CaCu_3Ti_4O_{12}$ (CCTO/SiO_2/CCTO) multilayered films were prepared on Pt/Ti/SiO_2/Si substrates by pulsed laser deposition method. It has been demonstrated that the dielectric loss and the leakage current density were significantly reduced with the increase of the SiO_2 layer thickness, accompanied with a decrease of the dielectric constant. The CCTO film with a 20 nm SiO_2 layer showed a dielectric loss of 0.065 at 100 kHz and the leakage current density of 6×10^{-7} A/cm^2 at 100 kV/cm, which were much lower than those of the single layer CCTO films. The improvement of the electric properties is ascribed to two reasons: one is the improved crystallinity; the other is the reduced free carriers in the multilayered films.

PACS: 73.21.AC; 81.15.Fg; 77.55+f

Keywords: A. Multilayers; B. Laser processing; D. Dielectric response

1. Introduction

With the shrinking of dimensions of the microelectronic devices, high dielectric constant materials play an important role in microelectronic devices such as capacitors and memory devices. Recent reports of colossal dielectric constant (CDC) have paid considerable attention to several new material systems, such as perovskite-related material $CaCu_3Ti_4O_{12}$ (CCTO) [1–8], nonperovskite material $Li_{0.05}Ti_{0.02}Ni_{0.93}O$ (LTNO) [9], percolative $BaTiO_3$–Ni composites [10], electron-doped manganites $Ca_{1-x}La_xMnO_3$ and hole-doped insulators $La_2Cu_{1-x}Li_xO_4$ and $La_{2-x}Sr_xNiO_4$ [11–13]. Of all these materials, CCTO is particular due to its weakly temperature-dependent dielectric constant in the frequency range between DC and 10^6 Hz. Compared with the high dielectric constants of most ferroelectric and relaxor materials, the values of more than 10^5 observed in CCTO, which do not show a ferroelectric transition or relaxor behavior, are extraordinarily high. Moreover, it has been accepted that the CDC in CCTO is not intrinsic. Subramanian et al. [2] and Sinclair et al. [3] reported that the internal barrier layer capacitor (IBLC) effect, originated from twin boundaries in single crystal or from grain boundaries in polycrystalline CCTO, is responsible for the CDC phenomenon. Lunkenheimer et al. [4] attributed the origin of the CDC to the interfacial polarization termed Maxwell–Wager relaxation, between the electrodes and the sample surface. Recently, our study revealed that both grain boundaries and electrode effects existed in the CCTO ceramic [14]. The CDC in CCTO was related to the ceramic itself, which was attributed from the grain boundaries effects. However, it may also partly originate from the electrode effects, which depended on the surface resistivity of the sample. Strong support for our results was provided by Zhang [15] in his work about the discrimination of the two effects. Through the measurement of ac conductivity for CCTO ceramic, the author demonstrated that the electrode and grain boundary acted as two depletion layers to induce the low-frequency dielectric relaxation and the high-frequency dielectric relaxation, respectively.

Even if the CDC in CCTO is not intrinsic, this material could be a possible candidate for applications as IBLC [16]. For realizing commercial application in integrated circuits, the thin film state for CCTO is the most possible one to be integrated into the current semiconductor technology,

* Corresponding author. Tel.: +86 512 6511 2251; fax: +86 512 6511 2597.
E-mail address: lfang@suda.edu.cn (L. Fang).

0038-1098/$ - see front matter © 2005 Elsevier Ltd. All rights reserved.
doi:10.1016/j.ssc.2005.12.004

compared with the crystal or ceramic [17–21]. However, one of the main problems for CCTO is its high dielectric loss and high leakage current, which make CCTO practically unusable. Up to now, few investigations have been done to solve the above problem. We note that in $Ba_{1-x}Sr_xTiO_3$ (BST) films, many efforts have been made to improve their electric properties by using a multilayered structure, such as BST/SiO_2 and BST/ZrO_2 multilayers [22,23]. Starting with the same idea, we propose that the artificially layered structure may offer opportunities to improve the electric properties of the CCTO films. In this paper, the multilayered films where a SiO_2 layer is interposed between two CCTO layers has been prepared on the Pt/Ti/SiO_2/Si substrates. It is expected that the CCTO/SiO_2/CCTO multilayered structure will exhibit low dielectric loss and leakage current while the dielectric constant keeps up in a useful range. The effect of the SiO_2 layer thickness on the electric properties of the CCTO films has been investigated.

2. Experimental detail

The CCTO/SiO_2/CCTO multilayered films were prepared by a multi-target pulsed laser deposition (PLD) technique. The PLD system consists of a KrF excimer laser (Lambda Physik 105i) with a 20 ns pulse width and wavelength of 248 nm, optical lens and a vacuum chamber system. The laser beam with a pulse repetition rate of 5 Hz was focused on the target through a quartz window with the laser energy density of 1.5 J/cm^2. Polycrystalline CCTO pellets and single crystal silicon wafer were used as targets for depositing CCTO and SiO_2 films, respectively. The Pt/Ti/SiO_2/Si substrates were placed parallel to the target at a distance of 3.5 cm and heated to 700 °C by a resistance heater. The chamber was first pumped down to 2×10^{-4} Pa, then oxygen was introduced to a pressure of 26.6 Pa. The films were deposited on substrates in sequence: first CCTO films, then SiO_2 films and finally CCTO films again. After deposition, the films were in situ annealed in the chamber at 700 °C in 0.5 atm oxygen atmospheres for 15 min and then cooled down to the room temperature. The thickness of the film was determined by an ET350 Talysurf profilometer (Kosaka Laboratory Ltd). In the sandwich structure, the intermediate SiO_2 layer had various thicknesses of about 5, 10 and 20 nm, respectively. Up- and down-CCTO layers had almost the same thickness (240 nm). For comparison, pure 480 nm CCTO films were also prepared by the same process. For carrying out the electrical measurements, Pt dots of 0.25 mm in diameter were deposited onto the top surface of the films at room temperature through a shadow mask by radio-frequency (RF) sputtering technique. The frequency-dependence of the dielectric properties was obtained using a HP4294A impedance analyzer over a frequency range of 100 Hz–2 MHz. The current–voltage (I–V) characteristics of the films were measured by a Keithley 2400 Source Meter.

3. Results and discussion

Fig. 1 shows the variation of dielectric constant and dissipation factor as a function of frequency for the CCTO and the CCTO/SiO_2/CCTO multilayered films. At 100 kHz, the dielectric constants and dielectric losses for the capacitors of Pt/CCTO/Pt, Pt/CCTO/SiO_2 (5 nm)/CCTO/Pt, Pt/CCTO/SiO_2 (10 nm)/CCTO/Pt and Pt/CCTO/SiO_2 (20 nm)/CCTO/Pt, were 983, 267, 171, 105, and 0.19, 0.084, 0.060 and 0.065, respectively. Obviously, the dielectric constants in all multilayered films were lower than that of the CCTO single layer films; however, the dielectric losses of the multilayered films also decreased, especially at the high frequency region. Similar phenomena were also observed in BST/SiO_2 multilayered films [22,24], and they can be explained using a simple two-layer model, in which a capacitor of CCTO is in series with a capacitor of SiO_2. Then, the dielectric constant of the CCTO/SiO_2/CCTO multilayer film can be calculated from the formula:

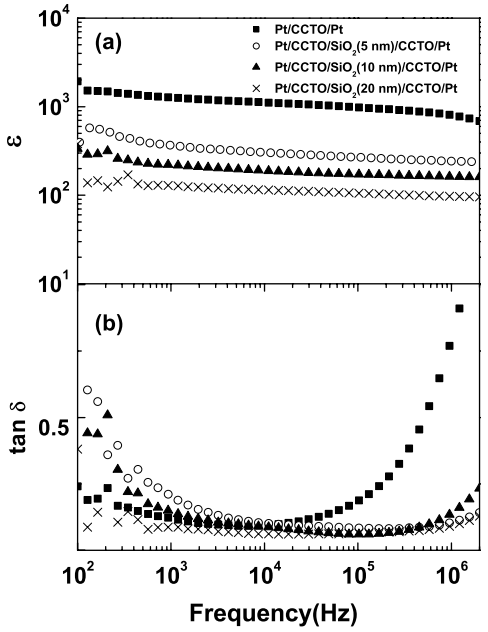

Fig. 1. Frequency dependence of (a) the dielectric constant and (b) the loss for the CCTO and the multilayer films.

$$\frac{d}{\varepsilon_r} = \frac{d_{CCTO}}{\varepsilon_{CCTO}} + \frac{d_{SiO_2}}{\varepsilon_{SiO_2}} \quad (1)$$

Where d is the total thickness of the CCTO/SiO_2 multilayer films, and d_{CCTO} and d_{SiO_2} are the thicknesses of the CCTO and SiO_2, respectively. ε_r is the dielectric constant of the multilayered films, whereas ε_{CCTO} is the dielectric constant of the CCTO films, which is about 980 in the study, and ε_{SiO_2} is the dielectric constant of the SiO_2, which is near 4. The ε_r calculated from Eq. (1) are 279, 162 and 88 for the different CCTO/SiO_2/CCTO multilayers with 5, 10 and 20 nm SiO_2 layer, respectively, which are close to the results of the experiment. However, as a simple hypothesis, it only provides us with a probable trend. The exact mechanism needs further researches.

Fig. 2 shows the leakage current density (J) vs electric field (E) data for the uniform and the multilayered films. The leakage current densities were recorded with both polarities of

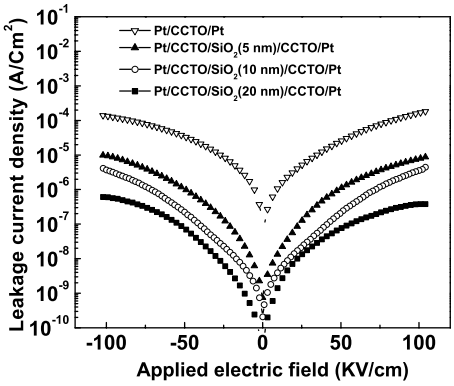

Fig. 2. Variation of leakage current density as a function of applied electric field for the CCTO and the multilayer films.

the applied electric fields on the top electrodes. No significant difference in leakage currents was observed when the bias was reversed. This is reasonable because the Pt/CCTO/SiO_2/CCTO/Pt capacitor system is completely symmetrical, and CCTO do not show ferroelectric behavior. Thus, applying voltage in direction or the other will be totally equivalent, regardless of whether the conduction is limited by interfacial barriers or by bulk-like mechanisms. Moreover, it was obvious in Fig. 2 that, at a given electric field, the leakage current density was considerably reduced by increasing the thickness of the SiO_2 layer. For instance, the leakage current density of the CCTO films with a 20 nm SiO_2 layer was around three orders of magnitude (6.0×10^{-7} A/cm^2 at 100 kV/cm), less than that of the single CCTO films (1.4×10^{-4} A/cm^2 at 100 kV/cm), showing much more resistive property.

In order to explore the mechanism behind the low dielectric loss and leakage current in the CCTO/SiO_2/CCTO multilayered films, we checked their microstructure by X-ray diffraction (XRD), recorded on a Rigaku diffractometer (D/MAX 3C) using Cu kα radiation at 40 kV. Fig. 3 shows the XRD results for the single layer CCTO and the multilayered films with a 10 nm SiO_2 layer. All the films were polycrystalline and showed the (220) and (422) peaks of the CCTO. The single layer CCTO films alone displayed a pattern with a strong (220) preferential orientation, which was consistent with our previous work [25]. As long as a thin layer of SiO_2 layer was interposed into the CCTO films, additional (211), (321) and (400) diffraction peaks were observed, implied the multilayered films are less well oriented and the (220) preferential orientation is completely relaxed. Similar phenomena were also observed in BST/SiO_2 multilayered films [22]. Furthermore, since the SiO_2 layer is only 10 nm, it is very difficult for us to observe the corresponding diffraction peaks in such multilayers. However, weak peaks could be observed near 20°, as shown in the left insert of Fig. 3(b), which may attribute to the phase of cristoballite SiO_2 [26]. The surface morphologies of the uniform and the multilayered films were also observed by a scanning probe microscope (NT-MDT Solver P47-PRO) operating in the contact atomic force microscope (AFM) over an area of 2×2 μm^2, as shown in the inset of Fig. 3. The root mean square (RMS) roughness of the multilayered films is 20.2 nm, which is smaller than that of the single layer CCTO films (27.9 nm). The single layer CCTO films formed directly on Pt/Ti/SiO_2/Si substrates exhibits nonuniform microstructure consisting of large grains and considerable volume fractions of micrograins, while the CCTO/SiO_2/CCTO multilayered films depict more small fine grains. From above, we note that the insertion of a SiO_2 layer in CCTO affects the crystallinity and surface morphologies of the films, which may be one reason for the improvement of the electric properties of the multilayers.

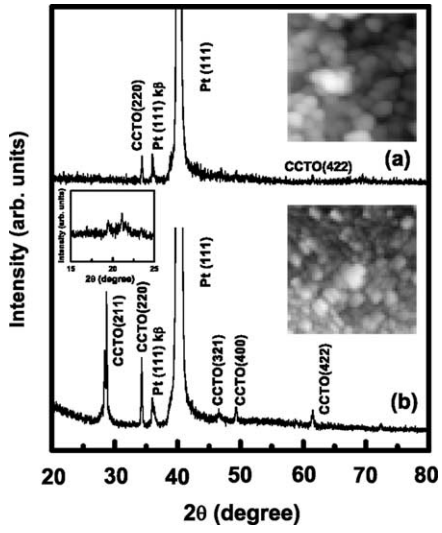

Fig. 3. X-ray diffraction patterns of (a) the single layer CCTO films (b) the CCTO/SiO_2 (10 nm)/CCTO films (The intensities are plotted on a linear scale). Inset shows the AFM micrographs (2×2 μm^2) of (a) the single layer CCTO films, (b) the CCTO/SiO_2 (10 nm)/CCTO films. Another left inset in (b) shows the fine scan around 20°.

It is well known that in most dielectric materials, the dielectric loss and leakage current density are related to the free carriers. The dielectric loss comes from two mechanisms [27]: the resistive loss and the relaxation loss of the dipole. In the resistive loss mechanism, the energy is consumed by free carriers in the film; while in the case of the relaxation loss mechanism, it is the relaxation of the dipole that expends energy. If there are free carriers in the films, the resistive loss is the dominant mechanism. As mentioned in our previous work [20,25], the CCTO thin films are usually fabricated under low oxygen pressures in order to improve the crystallinity and surface morphology. Under such kinds of thin film elaboration condition, space charge, such as oxygen vacancies, can be inevitably generated during the preparation of the films, according to the following reaction:

$$O_o(\text{oxygen ion at its normal site}) \rightarrow V_o(\text{oxygen vacancy}) + 2e^- + 1/2O_2$$

Such oxygen vacancies create deep energy level in the band gap for activated electrons to mobile. So, the more oxygen vacancies, the more free carriers can be generated in the films. Thus to investigate the free carrier existing in the films is also very useful for us to understand the mechanism behind the reduction of the dielectric loss and leakage current.

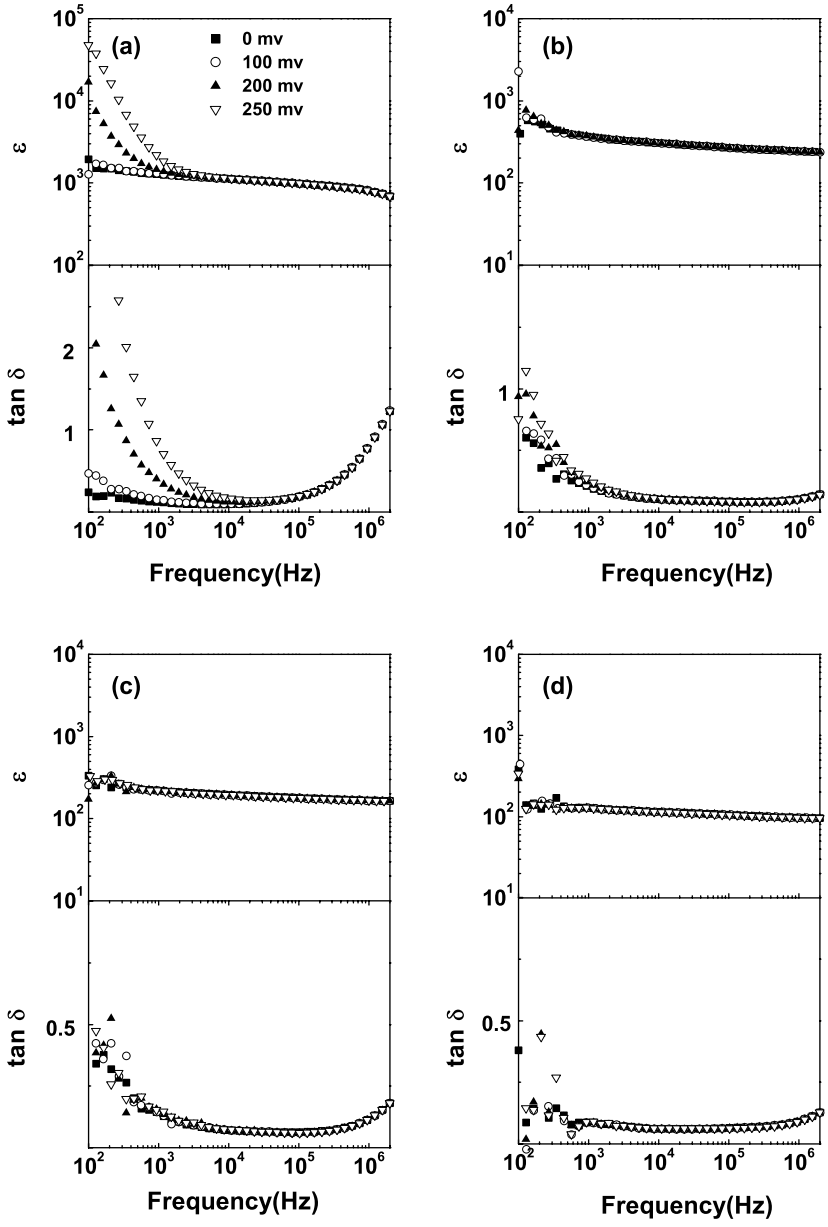

Fig. 4. Change of frequency characteristics of dielectric properties under different dc bias for (a) CCTO, (b) CCTO/SiO_2 (5 nm)/CCTO, (c) CCTO/SiO_2 (10 nm)/CCTO and (d) CCTO/SiO_2 (20 nm)/CCTO, respectively.

In order to check whether there are free carriers in the film, we added a dc bias on the top electrode during the measurements of dielectric properties. Fig. 4 presents the frequency dependence of the dielectric properties of the uniform and multilayered films with different dc voltages added on during the measurement. From Fig. 4(a), we note that the dielectric constant and dielectric loss of the Pt/CCTO/Pt capacitor below 10 kHz can be enhanced by dc bias, showing the low-frequency dielectric relaxation. Moreover, the larger the dc voltage is, the larger the dielectric enhancement can be obtained. These results indicate that there are free carriers existed in the single layer CCTO films. However, above phenomena disappeared gradually in the CCTO/SiO_2/CCTO multilayered films as the thicknesses of the SiO_2 layers increased, as shown in Fig. 4(b)–(d). This result implied that the number of free carriers decreased in the multilayered films. In CCTO/SiO_2/CCTO multilayered films, two additional interfaces between the CCTO and SiO_2 appeared in the structure. Similar to the case in the BST/ZrO_2 multilayers [23], we would expect the formation of the depletion layers at the CCTO/SiO_2 interfaces in the present multilayers. Such layers at the interface will have a higher electric field than the rest of the sample, which is more difficult for free carriers to transport.

In order to identify the assumption of the depletion layer, the main conduction mechanism in the CCTO and the multilayer films should be studied. Before characterizing the possible mechanism therein, several conduction mechanisms in thin films are first reviewed. One nonlinear conduction process is the space–charge-limited current (SCLC), corresponding to trap-free square law with self-blockage of charge carriers. Two

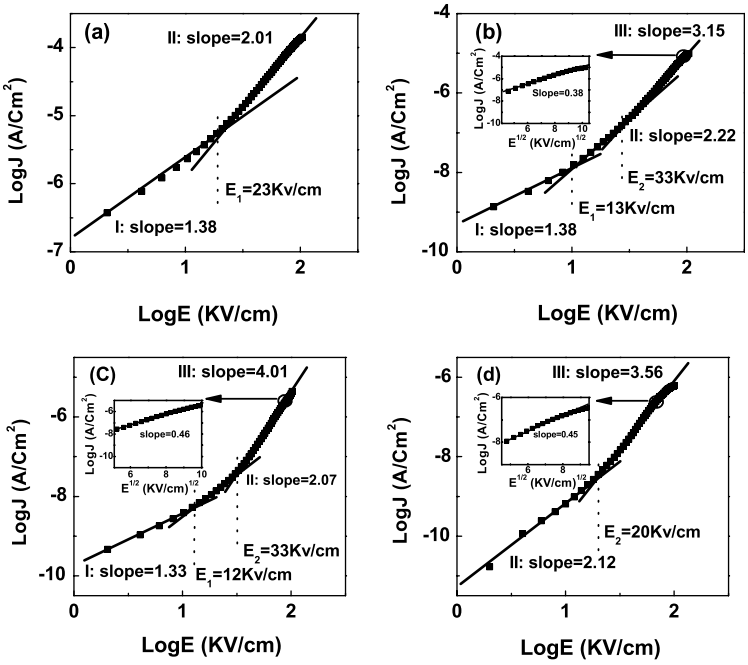

Fig. 5. The log J vs log E plots for (a) CCTO, (b) CCTO/SiO_2 (5 nm)/CCTO, (c) CCTO/SiO_2 (10 nm)/CCTO and (d) CCTO/SiO_2 (20 nm)/CCTO, respectively. The values of different slopes and transition field are listed in the plots. Insets are the plots of log J vs $E^{1/2}$ using the same set of data in the third slope region (denoted by arrow).

additional nonlinear conductions are called the field enhanced Schottky (ES) and Poole–Frenkel emission (PF). The former is also sometimes called interface controlled Schottky emission, which is a Schottky emission process across the interface between metal and an oxide films and always operates at low field. The latter is associated with the field enhanced thermal excitation of charge carriers from traps, sometimes called the internal Schottky effect, which always occurs at high field. These conductions mechanisms are very similar and can be determined from the slope measured from the straight line region of the J–E curve: The ES or PF emission can be expressed as Log J being proportional to $E^{1/2}$, While the SCLC J–E behavior exhibits $m=2$ (m is the slope of Log J–Log E) [28–31].

Fig. 5 shows the positively biased leakage current data in the form of Log J vs Log E for the uniform and the multilayered films. For the uniform films, the type of I–V clearly exhibits different slope regions. Initially, the leakage current shows an ohmic behavior due to the slope in close to 1 at a low electric field region less than 23 kV/cm, demonstrating that the volume conductivity is predominated in region I, which also indicate that the volume generated free carrier density, n_v, is higher than the injected free carrier density, n_i [29]. At higher electric field, the slope becomes 2.01 in region II, which agrees well with the SCLC theory, indicating that n_i exceeds n_v.

However, the insertion of SiO_2 barrier layer changes the conduction mechanisms of the CCTO thin films. As shown in Fig. 5(b) and (c), at low electric field, with the thickness of the SiO_2 barrier layer increasing, the transition field from ohmic behavior to SCLC behavior decreases (13 kV/cm for the case of 5 nm SiO_2, 12 kV/cm for the case of 10 nm SiO_2). Moreover, there is no ohmic behavior but only SCLC behavior in the CCTO films with 20 nm SiO_2 layer at low field (Fig. 5(d)), showing that such transition occurs at much lower field. Since, the state of injected free carrier density is not much changed due to the fact that the interfaces of the electrode/CCTO films are all present in both uniform and multilayered films. Such experiment phenomena are ascribed to the decrease value of n_v with the increase thickness of the SiO_2 layer, which is also consistent with the previous results of the dc bias dielectric properties measurement. In addition, for the multilayered films at high electric field, apart from region II, there exists another large slope region III. In this region, the conduction mechanism seems to be changed due to that in the Log J vs $E^{1/2}$ plot using the same set of data is reasonably linear (as seen in insets of Fig. 5(b)–(d)). In principle, both ES (which is interfacial) and PF (which is a bulk-like mechanism) can be expressed as Log J being proportional to $E^{1/2}$ [28–31], as mentioned above. However, since this region only appeared in the multilayered structures, we proposed that this phenomenon was originated from the interfacial barrier layers formed between CCTO and SiO_2.

4. Conclusion

In summary, CCTO/SiO_2/CCTO multilayered films with different thicknesses of SiO_2 layers were prepared on Pt/Ti/SiO_2/Si substrates by PLD method. Comparing with the uniform CCTO films, the dielectric loss and the leakage current density in the multilayered films were reduced dramatically with the increasing thickness of SiO_2 layer, accompanied with a reduction of the dielectric constant. The microstructure and

the conduction mechanism have also been investigated. The improvement of the electric properties is ascribed to the improved crystallinity and the reduced free carriers in the multilayered films.

Acknowledgements

This research was supported by the National Natural Science Foundation of China (Grant No. 10204016).

References

[1] C.C. Homes, T. Vogt, S.M. Shapiro, S. Wakimoto, A.P. Ramirez, Science 293 (2001) 673.
[2] M.A. Subramanian, L. Dong, N. Duan, B.A. Reisner, A.W. Sleight, J. Solid State Chem. 151 (2000) 323.
[3] T.B. Adams, D.C. Sinclair, A.R. West, Adv. Mater. 14 (2002) 1321.
[4] P. Lunkenheimer, V. Bobnar, A.V. Pronin, A.I. Ritus, A.A. Volkov, A. Loidl, Phys. Rev. B 66 (2002) 052105.
[5] M.H. Cohen, J.B. Neaton, L.X. He, D. Vanderbilt, J. Appl. Phys. 94 (2003) 3299.
[6] L. Zhang, Z.J. Tang, Phys. Rev. B 70 (2004) 174306.
[7] S.Y. Chung, I.D. Kim, S.J.L. Kang, Nat. Mater. 3 (2004) 774.
[8] S.V. Kalinin, J. Shin, G.M. Veith, A.P. Baddorf, M.V. Lobanov, H. Runge, M. Greenblatt, Appl. Phys. Lett. 86 (2005) 102902.
[9] J.B. Wu, C.W. Nan, Y.H. Lin, Y. Deng, Phys. Rev. Lett. 89 (2002) 217601.
[10] C. Pecharromán, F. Esteban-Betegón, J.F. Bartolomé, S. López-Esteban, J.S. Moya, Adv. Mater. 13 (2001) 1541.
[11] J.L. Cohn, M. Peterca, J.J. Neumeier, Phys. Rev. B 70 (2004) 214433.
[12] T. Park, Z. Nussinov, K.R.A. Hazzard, V.A. Sidorov, A.V. Balatsky, J.L. Sarrao, S.W. Cheong, M.F. Hundley, J.-S. Lee, Q.X. Jia, J.D. Thompson, Phys. Rev. Lett. 94 (2005) 017002.
[13] J. Rivas, B. Rivas-Murias, A. Fondado, J. Mira, M.A. Señarís-Rodríguez, Appl. Phys. Lett. 85 (2004) 6224.
[14] J. Yang, M.R. Shen, L. Fang, Mater. Lett. 59 (2005) 3990.
[15] L. Zhang, Appl. Phys. Lett. 87 (2005) 022907.
[16] P. Lunkenheimer, R. Fichtl, S.G. Ebbinghaus, A. Loidl, Phys. Rev. B 70 (2004) 172102.
[17] Y. Lin, Y.B. Chen, T. Garret, S.W. Liu, C.L. Chen, L. Chen, R.P. Bontchev, A. Jacobson, J.C. Jiang, E.I. Meletis, J. Horwitz, H.D. Wu, Appl. Phys. Lett. 81 (2002) 631.
[18] W. Si, E.M. Cruz, P.D. Johnson, P.W. Barnes, P. Woodward, A.P. Ramirez, Appl. Phys. Lett. 81 (2002) 2058.
[19] A. Tselev, C.M. Brooks, S.M. Anlage, H. Zheng, L.S. Riba, R. Ramesh, M.A. Subramanian, Phys. Rev. B 70 (2004) 144101.
[20] L. Fang, M.R. Shen, W.W. Cao, J. Appl. Phys. 95 (2004) 6483.
[21] R.L. Nigro, R.G. Toro, G. Malandrino, M. Bettinelli, A. Speghini, I.L. Fragala, Adv. Mater. 16 (2004) 891.
[22] V. Reymond, D. Michau, S. Payan, M. Maglione, J. Phys.: Condens. Matter 16 (2004) 9155.
[23] S.K. Sahoo, D.C. Agrawal, Y.N. Mohapatra, S.B. Majumder, R.S. Katiyar, Appl. Phys. Lett. 85 (2004) 5001.
[24] L.Z. Cao, B.L. Cheng, S.Y. Wang, Y.L. Zhou, K.J. jin, H.B. Lu, Z.H. Chen, G.Z. Yang, J. Appl. Phys. 98 (2005) 034106.
[25] L. Fang, M.R. Shen, Thin Solid Films 440 (2003) 60.
[26] L.A. García-Cerda, O.M. González, J.F. Pérez-Robles, J.G. Hernández, Mater. Lett. 56 (2002) 450.
[27] P. Li, J.F. McDonald, T.M. Lu, J. Appl. Phys. 71 (1992) 5596.
[28] S.Y. Wang, B.L. Cheng, C. Wang, S.Y. Dai, H.B. Lu, Y.L. Zhou, Z.H. Chen, G.Z. Yang, Appl. Phys. Lett. 84 (2004) 4116.
[29] X. Qi, J. Dho, R. Tomov, M.G. Blamire, J.L.M. Driscoll, Appl. Phys. Lett. 86 (2005) 062903.
[30] S. Ezhivalavan, V. Samper, T.W. Seng, J.M. Xue, J. Wang, J. Appl. Phys. 96 (2004) 2181.
[31] T.L. Chen, X.M. Li, W.B. Wu, W.D. Yu, X.D. Gao, X. Zhang, Appl. Phys. Lett. 86 (2005) 132902.